İSTANBUL UNIVERSITY PRESS

Coğrafya Dergisi
Journal of Geography

Coğrafya Dergisi–Journal of Geography
JGEOGRAPHY 2025, (51): 146–158

https://doi.org/10.26650/JGEOG2025-1759348

Submitted: 14.02.2024
Revision Requested: 14.03.2024
Last Revision Received: 18.03.2024
Accepted: 02.04.2024
Published Online 27.05.2024

Research Article

Open Access

Paleoclimatic Reconstruction Based On Multi-Proxy Data Obtained From The Lake Sediments In Aşağı Pınar Region (Kırklareli, Türkiye): Preliminary Results

Özlem Yurtseven Uyar [1], Hüseyin Turoğlu [2], AhmetEvren Erginal [3] & Nurettin Yakupoğlu [4]

[1] Istanbul University, Institute of Social Sciences, Department of Geography, Istanbul, Türkiye.
[2] Istanbul University, Department of Geography, İstanbul, Türkiye.
[3] Çanakkale Onsekiz Mart University, Department of Geography Education, Çanakkale, Türkiye.
[4] Istanbul Technical University, Faculty of Mines, Geological Engineering, İstanbul, Türkiye.

Abstract

The uncertainties of the paleoclimatic conditions and changing characteristics of Eastern Thrace, due to its remarkable geographical location serving as a stage for inter-regional interaction and its importance for cultural history, remain a critical area of scholarly investigation. While analytical research on this topic is limited, scholarly inquiry into past climatic features based on multi-element and mineral analyses and their proportional distributions, organic carbon, and $CaCO_3$ analyses is conspicuously absent from the current literature. This study aims to examine the geochemical indicators of an ancient lake sediment sequence located in the Aşağı Pınar region, 5 km south of the city centre of Kırklareli (Türkiye), to reconstruct the past climatic features and changes in the region.

To do so, the sedimentary geometry and suitable drilling location of the proxy trap containing the sedimentary data of this paleoenvironment were determined using the electrical resistivity tomography (ERT) method. A total of 147 samples of the drill core are analysed using $CaCO_3$(%), TOC (%), X-ray diffraction (XRD) as well as inductive coupling plasma–mass spectrometry (ICP-MS). The distinct samples at the reference level were examined through AMS^{14}C dating.

The results revealed that rainy and dry periods are defined based on the fluctuations across mineral composition, multi-element analyses, and index calculations; further, the geochemical data yield five different periods characterised by distinctive temperature and humidity conditions. The radiocarbon dating results that the analysed sedimentation was dated between 36,854±233 years BP. Offering a novel database specific to the region, this study deepens our understanding of the region's historical and civilizational significance.

Keywords Paleoclimate · Multi-Proxy Data · Lake Sediments · Eastern Thrace.

Citation: Uyar, Ö Y., Turoğlu, H, Erginal, A & Yakupoğlu, N (2025). Aşağı Pınar Bölgesi (Kırklareli, Türkiye) Göl Sedimentlerinden Elde Edilen Çoklu Gösterge Verilerine Dayali Paleoklimatik Rekonstrüksiyon: Ön Bulgular. *Coğrafya Dergisi–Journal of Geography*, (51), 146-158. https://doi.org/10.26650/JGEOG2025-1759348

This work is licensed under Creative Commons Attribution-NonCommercial 4.0 International License.

© 2025. Uyar, Ö. Y., Turoğlu, H., Erginal, A. & Yakupoğlu, N.

Corresponding author: Özlem Yurtseven Uyar ozlemyurtsevenuyar@ogr.iu.edu.tr

INTRODUCTION

Different scientific methodologies and data sources are employed to determine the short- and long-term changes in past climatic conditions. With the advent of advanced analytical techniques, paleolimnological studies based on multi-proxy analyses are demonstrating increasing prominence and significance within the contemporary academic discourse due to their ability to provide high-resolution data (Birks & Birks, 2006; Gayantha et al., 2017; Schroeter et al., 2020; Danladi et al., 2023). Scholarly interest in lake sediments has also increased because they not only enable understanding of past changes in temperature, precipitation, and vegetation but also reveal the complex interactions between climatic changes and human activities.

A substantial body of literature has investigated Quaternary climate changes based on the paleoenvironmental records of sediments from different lakes across Anatolia (Roberts et al., 2001; Jones et al., 2006; Eastwood et al., 2007; Turoğlu, 2007; England et al., 2008; Jones and Roberts, 2008; Turoğlu et al., 2008; Leroy et al., 2010; Kuzucuoglu et al., 2011; Turoğlu, 2011; Ocakoğlu, 2013; Erginal et al., 2017; Kılıç et al., 2018; Inkaya et al., 2025). Binary ratio analyses based on element ratios such as Ca/Fe and Fe/Mn, which are widely used in the international paleolimnology and geochemistry literature, have not yet been performed for lake/river/swamp sediments in Eastern Thrace. Geochemical studies in the region have primarily focused on hydrocarbon potential (Gürgey, 2009), mineralisation (Sezen & Karakaş, 2025) and heavy metal pollution (Dökmeci, 2017), leaving a scientific gap in the use of multi-element data as paleoclimatic proxies.

While studies based on fossil pollen and isotope data have been conducted across Eastern Thrace, the distribution of proxy elements of detrital and authigenic origin in lake sediments in this region remains relatively understudied. Remarkably, the existing body of research fails to include trends in proxy elements, such as the element abundance ratios of Ca/Fe, Ca/Ti (Roeser et al., 2012; Çağatay et al., 2014) and Rb/Sr (Jin et al., 2001; Jin et al., 2006; Von Gunten et al., 2009; Hu et al., 2010; Liu et al., 2014; Minyuk et al., 2014), which are widely used to assess the climate-controlled accumulation of lake sediments.

Aşağı Pınar (Kırklareli/Türkiye) is the archaeological settlement that best represents prehistoric life in Thrace (Özdoğan, 2015). Located on a relatively high ridge compared to its surroundings, the Aşağı Pınar archaeological settlement is considered to have been a waterfront (lake) settlement in prehistoric times (Özdoğan, 2011a; Özdoğan, 2011b; Özdoğan, 2015). Today, the traces of the Aşağı Pınar paleo-lake in the morphology have been almost completely erased. In archaeological settlements, the concept of 'interaction area' or 'interaction basin" is understood to mean that agricultural communities used areas within an average walking distance of one hour or within a 5 km radius, while pastoral communities used areas within an average walking distance of 1.5 hours or within a 7.5 km radius (Vita-Finzi et al., 1970; Vita-Finzi, 1978; Roper, 1979). Paleo-Lake is expected to be located within a 1-h walking distance of the Aşağı Pınar prehistoric settlement, as it is an important natural resource for the Aşağı Pınar archaeological site. Based on this approach, the area within a one-hour walking distance (5 km radius) of the archaeological settlement was investigated by jointly evaluating its geomorphology, lithology, soil, and vegetation characteristics. It was predicted to be an ancient lakebed plain (Figure 1; Figure 2).

The study area is referred to as the Aşağı Pınar region, within the interaction area of the Aşağı Pınar prehistoric settlement. The Aşağı Pınar region is located in Eastern Thrace, a few kilometres south of the centre of Kırklareli province of Türkiye (41º43'12" N – 27º13'31" E, elevation: 200m ±50 m) (Figure 1). The Istranca (Yıldız) Mountain of metamorphic rocks, extending roughly in the east-west direction in the north and reaching an altitude of 1031 m (Mahya Hill), forming an important morphological feature. The Istranca Mountain acts as a barrier, preventing the climatic influence of the Black Sea from reaching the study area, ensuring that the Aşağı Pınar region and its surroundings remained under continental climate conditions. The investigation area is located on a low plateau consisting of carbonate rocks, with a topographic slope towards the south and divided by a parallel to subparallel drainage pattern (Figure 1).

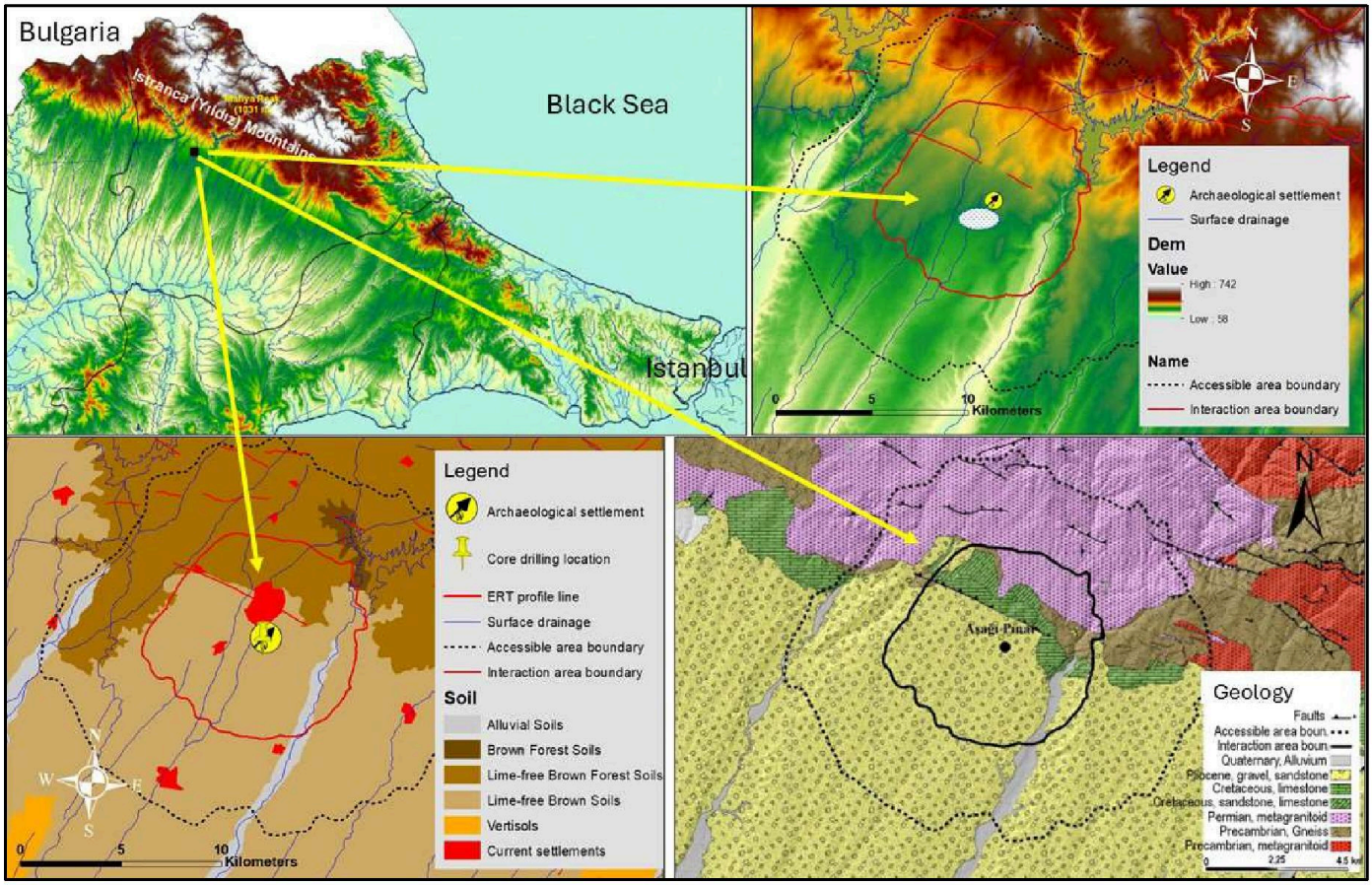
This study aims to draw inferences based on the vertical cumulative distribution and binary proportional distribution of proxy elements pertaining to the sediments of the Aşağı Pınar Lake (as till-water body), and thus to present a paleo-climatological reconstruction by correlating the findings through age-depth analysis.

Due to the geographical location of the investigation area, the region has become extremely susceptible to climatic fluctuations from the past to the present. This makes the old Aşağı Pınar Lake and its sediments a rare proxy trap in the region and a valuable resource for paleoclimatic inferences. The results of this study, based on proxy data obtained from the lake (still water) sediment, will aim to fill critical knowledge gaps that are essential for understanding the Late Quaternary climatology of the region. This research also holds the distinction of being the first to understand the Eastern Thrace Late Quaternary Palaeoclimatology through

Figure 1
Location map of the study area.



Figure 2
Geological, morphological, surface drainage, and soil characteristics maps of the ERT profile lines, drilling locations, and surrounding area.



an approach based on the determination of paleoclimatic changes and their timing using selected proxy elements (Ca, Sr, Na, Mg, Fe, Rb, K, Al, Ti, Zr, Be), autigenically precipitated calcium carbonate ($CaCO_3$), total organic carbon (TOC), and mineral crystal structure determination. This research, which defines paleoclimatic processes based on a new and original database specific to the region, is also significant in terms of its potential to contribute to the interpretation of the

region's prehistoric living environment from a geographical perspective.

METHODS

This study employed multiple electrical resistivity tomography (ERT) measurements to assess whether the area, which was previously considered as a paleo-lake area based on geomorphological and paedological field observations, is a proxy trap and to ascertain the appropriate drilling location. Furthermore, this study conducted 2D inverse solution measurements in Wenner Schlumberger arrays, evaluated the field data using RES2DINV software, and determined the horizontal and vertical distribution of the fine-grained sedimentary sequence. The investigation with ERT helped identify suitable drilling locations, and sediment samples were collected using a full hydraulic drilling rig. Based on the depth-dependent soil properties, suitable lake sediments were retrieved for the proxy data and transferred to a sterile container. In addition, a second drilling was carried out 10 m north of the first drilling location for verification and validation purposes, and a second set of cores from the paleo-lake sediments was taken from the sequence. After the sedimentological analysis of the cores, the relevant samples were classified and prepared for laboratory analysis.

For the proxy data, 147 samples, one taken every 10 cm, were cut from the drill core. This study examined the carbonate ($CaCO_3$), total organic carbon (TOC), mineral, and multi-element content of the samples. More specifically, the $CaCO_3$ and TOC contents of all 147 samples were analysed, and reference levels for the inverse relationship between carbonate precipitation and organic carbon were identified based on the results.

The calcium carbonate content of the sediment samples was calculated as a percentage (%) based on the measurement of CO_2 volume with a Scheibler calcimeter (Schlichting & Blume, 1966). This method involves measuring the volume of CO_2 gas (in cm^3) formed in the reaction of carbonate compounds with hydrochloric acid (HCl). TOC determination revolves around the oxidation of organic matter by dichromate in an acid medium. For oxidation, potassium dichromate was reacted with iron sulphate and the resulting mixture was then titrated with potassium permanganate (Smith & Weldon, 1941).

Crystal structure analysis was performed using the XRD method on the sections of the core that indicated arid climate conditions to identify the origin of $CaCO_3$ precipitation. The key difference between calcite and aragonite, which have the same chemical composition as polymorphs of natural calcium carbonate, is their crystal system and the conditions of their precipitation (Rossi & Lozano, 2016; Roeser et al., 2016; Febrida et al., 2021). X-rays, which have energy levels higher than ultraviolet light but lower than gamma rays, were directed at the sample using the XRD method, and diffraction and dispersion data were collected to identify these polymorphs. X-ray measurements constitute a powerful method that provides information about the structure of the crystal without causing any damage to it.

Determining the mineral and elemental composition of the environment is significant because it reflects the sedimentation conditions and the underlying climatic factors (Erginal et al., 2017). This study is based on the principle that the carbonate ratio in lake sediments changes with increasing air temperature and rainy periods. Furthermore, this study posits that another source of increased carbonate could be allochthonous carbonate clasts from the drainage basin and the disintegration of biogenic carbonate skeletons. During the assessment of the analysis results, particular attention was given to whether the Ca concentration oscillated in the same direction as the other elements. If Ca varies in the same direction as the other elements, this implies that they are transported together, while a divergence from the elements transported by terrestrial inflow indicates that Ca refers to the proportion of calcium carbonate that precipitates by evaporation (Dean, 1999; Rostási et al., 2022). For this reason, the elements Si, Mg, Ti, Al, Ca, Sr, Rb, Fe, K, and Na were analysed for multi-element determination by inductively coupled plasma-mass spectrometry (ICP-MS).

The ICP-MS method is a mass spectrometry-based method that can determine elements both qualitatively and quantitatively and identify isotopes. This process involves ionising the sample, usually in a solution, with an inductively coupled plasma (Ar plasma) and then using a mass spectrometer to separate and measure these ions based on their mass-to-charge (m/z) ratio. The detection limit for many elements in the ICP-MS method is lower than parts per billion (ppb). This makes it the most convenient method for determining the quantity of the trace elements.

The binary proportional distribution method refers to analyses that use the ratios of two elements (e.g., Fe/Mn, Ti/Al, Sr/Ca). Palaeoenvironmental or sedimentological interpretations were made based on the relationships between the element ratios. The study examined the accumulation trends of proxy elements with depth and the ratios of these elements to one another. Based on these data, paleoenvironmental conditions and paleoclimatic inferences were made. In this context, the trends of the elements as well as their ratios to each other were used to determine the climatic arid and humid phases. High Fe/Ti ratios are associated with high precipitation conditions due

to terrestrial transport. Lithophile elements are considered as indicators of regional input to the ancient lake environment and are also used for normalisation purposes in carbonate sedimentation studies.

Reference levels indicating environmental changes are interpreted through the age-depth model (Blaauw, 2010; 2022) using the dating data obtained via the AMS ^{14}C method. Age–depth modelling was performed using the Clam package (Blaauw, 2010) in R version 4.4.2. The model applies a non-Bayesian (classical) approach based on interpolation between calibrated ^14C ages. The uncertainty ranges and ± values represent the 95% confidence intervals (2σ) derived from the probability distributions of the calibrated radiocarbon ages and propagated through the age–depth interpolation process.

FINDINGS

Geoelectrical Imaging Survey

Considering the morphological, soil, and natural vegetation characteristics of the agricultural area and its surroundings near the Aşağı Pınar prehistoric settlement, it was predicted that this plain could be the paleo-lake bottom. Three different ERT profile lines were identified to test the accuracy of this prediction (Table 1; Figure 3). ERT measurement results were used to detect underground resistivity anomalies, identify areas containing paleoenvironment proxies and suitable deposits for sampling, and determine drilling locations. The three multiple electrical resistivity tomography (ERT) surveys performed in the investigation area (Figure 3) employed a geo-electrical installation cable with a profile length of 144 metres and an electrode spacing of 3 metres, using 48 electrodes. Table 1 includes the coordinates of the multi-electrode resistivity measurements performed in the investigation area (Figure 3).

Figure 3

Profile lines of ERT 1, ERT 2, and ERT 3, along with the drilling location.



Along the ERT-1 profile, a depth of approximately 24 metres was identified from the surface (Figure 4). The results indicate a range of resistivity values from 4.07 to 65.4 ohm.m. The lithologic and stratigraphic characteristics were examined; the analysis yielded low-resistivity units (Figure 4: light and dark blue-coloured areas) with a resistivity range of 4.07 to 9.00 ohm.m, extending from the beginning to the end of the survey line at a depth of 2 metres and occasionally reaching 18 metres. These stacked units correspond to the clay. This accumulation zone, with its high moisture content and fine-grained organic sediment structure, is consistent with the core data. For the units with a resistivity range of 13.4 to 19.9 ohm.m (Figure 4: light and dark green-coloured areas), the uppermost layer is considered to be the fill topsoil, while the lowermost layer is interpreted as lacustrine silt, sand, and clay sediments. The units with a resistivity range of 29.6 to 65.4

Table 1

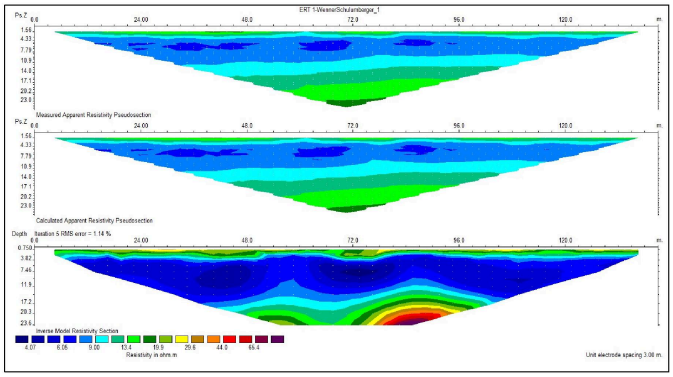
Installation coordinates for multiple electrodes.

Profile No.	Beginning		End		Electrode Spacing(m)	Profile Length(m)
ERT-1	2772633E	2007235 N	2772668E	2007384 N	3	144
ERT-2	2772592E	2007294 N	2772671E	2007425 N	3	144
ERT-3	2772605E	2007266 N	2772580E	2007418 N	3	144

ohm.m between 75 metres to 102 metres along the survey line and at depths ranging from 18 to 24 metres (Figure 4: yellow-red-purple-coloured areas) correspond to weathered, detrital, and fractured limestone, consistent with the core data.

Figure 4

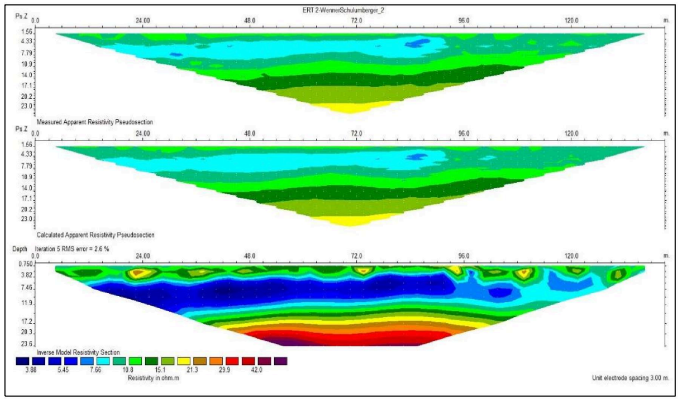
ERT-1 line and 2D ERT resistivity profiles.



The ERT-2 profile (Figure 5), reaching a depth of approximately 24 metres from the surface, exhibits resistivity values ranging between 3.88 and 42.0 ohm.m. The low-resistivity units (Figure 5: light and dark blue-coloured areas) with a resistivity range of 3.88 to 7.66 ohm.m, extending from the beginning to the end of the survey line at a depth of 2 metres and occasionally reaching 16 metres, correspond to clay deposits. The units with a resistivity range of 10.8 to 15.1 ohm.m (Figure 5: light and dark green-coloured areas) are interpreted as silt, sand, and clay sediments underlain by the fill topsoil. The units with a resistivity range of 21.3 to 42.0 ohm.m between 37 metres to 102 metres along the survey line and at depths ranging from 18 to 24 metres (Figure 5: yellow-red-purple-coloured areas) correspond to weathered, detrital, and fractured limestone.

Figure 5

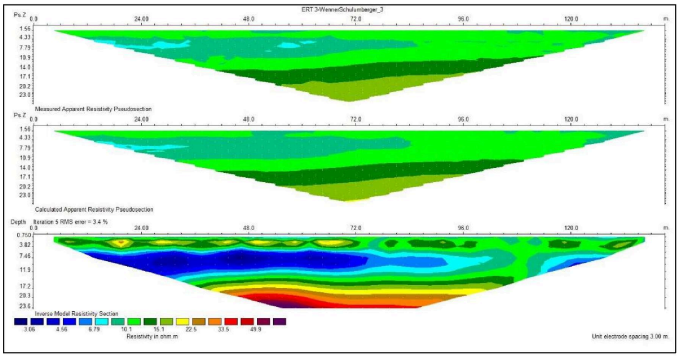
ERT-2 line, 2D ERT resistivity profiles.



The resistivity values of the ERT-3 profile (Figure 6) range between 3.06 and 49.9 ohm.m. The lithologic and stratigraphic characteristics were analysed, revealing low-resistivity units (Figure 6: light and dark blue-coloured areas) with a resistivity range of 3.06 to 6.79 ohm.m, extending from the beginning to the end of the survey line at a depth of 4 metres and in some instances, reach of 16 metres. These stacked units correspond to the clay deposits. The units with a resistivity range of 10.1 - 15.1 ohm.m (Figure 6: light and dark green-coloured areas) in the ERT-3 profile, the uppermost layer corresponds to the fill topsoil, while the lowermost layer corresponds to the silt, sand, and clay sediments. The units with a resistivity range of 22.5 to 49.9 ohm.m from 36 metres to 100 metres along the survey line and at depths of 18 to 24 metres (Figure 6: yellow-red-purple-coloured areas) correspond to weathered, detrital, and fractured limestone.

Figure 6

ERT-3 line, 2D ERT resistivity profiles.



At the 70th metre of the ERT-1 line, core drilling penetrated the bedrock at 21.00 m (Figures 3 and 7). The drilling log indicates that the top 1 m from the surface consists of soil disturbed by agricultural activities. The 1.00-4.00 m zone consists of silty clay of a yellowish light brown colour. This zone represents a well-oxygenated, relatively low to medium organic matter content, fine-grained deposit. A dark grey-greenish clay zone cuts the 4.00-16.00 m zone. The dark grey-green colour in the lake deposit indicates that the lake sediments are rich in iron and organic matter (Sebag et al., 2013; Strakhovenko et al., 2020; Łachacz et al., 2024). At depths of 16.00-20.50 m, a zone of beige sandy clay, sand, and limestone fragments is intersected towards the depth. The drilling terminated in the limestone bedrock (Figure 7). The drilling data and ERT findings corroborate each other.

Figure 7

Core drilling log taken at the 70th metre of the ERT-1 line.

Depth (m)	Ground definition
0,00 – 0,99	Soil
1,00 – 3,99	Yellowish brown silty clay
4,00 – 15,99	Grey-green coloured hard clay
16,00 – 20,49	- Beige-coloured sand, - Limestone fragments, - Limestone
20,50 – 21,00	Limestone (end of drilling)

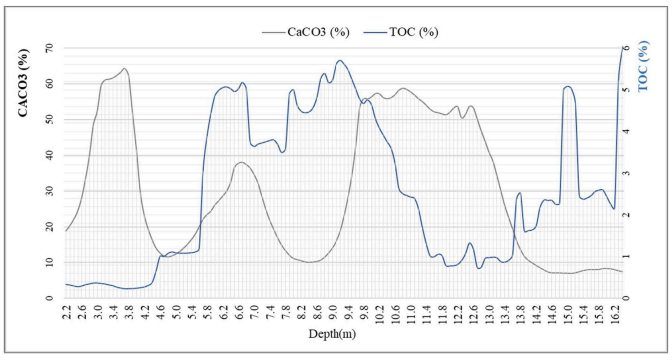


Variations and Trends in the Proxy Data Concentrations

The carbonate ratios (%) of the Aşağı Pınar paleo-lake were examined; the results show that the values varied from 5.93% to 91.98%, with an average of 34.15% (Figure 8). The high calcium carbonate ratios that this area may have functioned as a closed basin in the past. The points on the graph where the calcium carbonate ratio is elevated indicate an environment with arid climate conditions characterised by low weathering rates and severe erosion. The points on the graph where the calcium carbonate ratio is decreased, conversely, lower calcium carbonate ratios correspond to humid climatic conditions and a rapid weathering environment (Dean, 1999; Rostási et al., 2022). Although the depth-dependent variation of the calcium carbonate ratios provides initial reference levels, they are insufficient for detailed paleoclimatic interpretations. Considering that this sedimentation may have occurred authogenically through evaporation or organic production or may be of a detrital source through transport from the host rock, its high concentration alone is not necessarily a direct indicator of arid conditions. Therefore, a high carbonate content is not necessarily an indicator of arid climatic conditions. Here, ascertaining the sediment's origin is important for understanding the paleoclimatic conditions. Therefore, this study evaluates the relationship between calcium carbonate and total organic carbon, as well as the correlation between Ca and elements transported by terrestrial flow—such as Fe, Zr, and Ti—through mineralogical and multi-element analyses and discusses the results in the relevant sections.

Figure 8

Changes in carbonate and TOC with depth (%).



TOC (Total Organic Carbon) is considered an indirect measure of the amount of organic matter stored in the lake sediments. High TOC values generally indicate high primary production (production of organic matter by photosynthetic organisms) in lakes (Hedges & Keil, 1995; Dean, 1999; Meyers, 2003). The minimum and maximum total organic carbon (TOC) values of the Aşağı Pınar paleo-lake were found to range from 0.09% to 7.88% in the sediment analysed by the Smith-Weldon method (1941). Another key finding was that, of the 147 samples taken every 10 cm from the core, 36 samples had very low organic matter content (0-1%); 13 samples had low content (1-2%); 10 samples had moderate organic matter content (2-3%); 23 samples had good content (3-4%), and 65 samples had high organic matter content (>4%). Notably, approximately half of the sediment samples (44%) displayed a very high concentration of organic matter.

This suggests that during the sedimentation process in the study area, the water mass overlying the sediment was rich in microorganisms and had excessive primary biological productivity. The preservation of microorganisms during primary productivity in the sediment can be attributed to an oxygen-free (anaerobic) environment (Dean, 1999; Meyers, 2003). The grain size of the deposited sediment was also found to play a significant role. Indeed, as the grain size decreases, the organic matter retention increases with increasing surface area, and the oxygen mobility within the sediment decreases, resulting in an increased amount of organic matter in the sediment. The richness of the sediment in the investigation area in terms of organic matter is linked to the density of the clay-sized material as well as the primary productivity. Levels characterised by abundant organic matter reflect relatively rainy and humid climatic conditions, whereas levels with low organic matter indicate cold-arid paleoclimate conditions in the depositional environment. On the other hand, levels characterised by low organic carbon and high carbonate content indicate that sedimentation occurred under a closed drainage system and conditions (Hedges & Keil, 1995; Dean, 1999). The correlation value (R^2: 0.13) shows a very low positive correlation, if not negative, which means that the carbonate was precipitated by evaporation, not classically (Table 2). To investigate the cause of the carbonate precipitation at 3.60 and 12.20 metres, which indicates arid climatic conditions, crystal structure determination was conducted using the XRD method, and the polymorphs of $CaCO_3$ were analysed.

Both calcite and aragonite share the same chemical composition as the polymorphs of natural calcium carbonate ($CaCO_3$), but their key differences lie in their crystal systems and depositional environments. The precipitation of calcite, a mineral commonly observed in various sediments and sedimentary rocks, is associated with water and/or soil evaporation. This process occurs when calcium carbonate becomes saturated in water due to increasing water temperature and pH changes, followed by the formation of a nucleus (nucleation) of its ions and the accumulation of growing crystals in the sedimentary environment. As a

Table 2

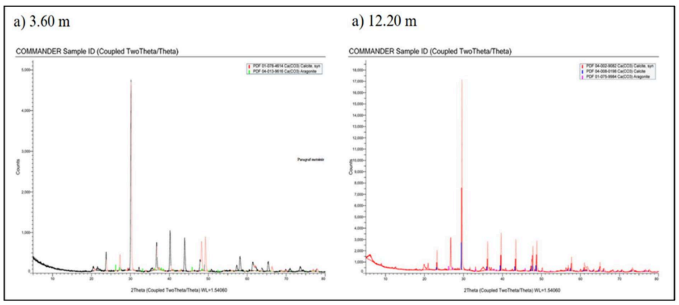
Results of the $CaCO_3$ and TOC Regression Analysis

Regression Statistics						
Multiple R	0,366434395					
R Square	0,134274166					
Adjusted R Square	0,109887522					
Standard Error	4,068041376					
Observations	74					
ANOVA						
	d	*SS*	*MS*	*F*	*Significance F*	
Regression	2	182,2389297	91,1194649	5,50605363	0,005984163	
Residual	71	1174,976205	16,5489606			
Total	73	1357,215135				
	Coefficients	*Standard Error*	*t Stat*	*P-value*	*Lower %95*	*Upper %95*
Intercept	7,811022928	1,31165169	5,95510454	9,04408E-08	5,19566374	10,42638212
Variable X 1	−0,018135366	0,021008585	−0,86323595	0,390914456	−0,060025294	0,023754563
Variable X 2	0,547330669	0,213197738	2,56724426	0,012358852	0,122226454	0,972434885

result, the density of calcite indicates periods characterised by hot and arid climate conditions (Kıyak & Erginal, 2010). In contrast, aragonite precipitates in colder and wetter climatic conditions. The crystallisation of aragonite takes longer, and cold, humid conditions allow calcium carbonate ions to remain in the sediment for extended periods. For this reason, the aragonite concentration indicates the presence of low pressure, low temperature, and a humid environment during sedimentation (Rossi & Lozano 2016; Roeser et al. 2016). The analysis of both levels (the depths of 3.60 and 12.20 metres) shows that calcite, which is a proxy for drought, predominated (Figure 9). This can be attributed to the precipitation occurring during the hot and dry periods, which results in high evaporation. When compared to the calcium carbonate graph of the core (Figure 8), a sudden increase in $CaCO_3$ was observed at the relevant depths, which is notable. Thus, it is plausible to argue that the results of both analyses support each other.

Figure 9

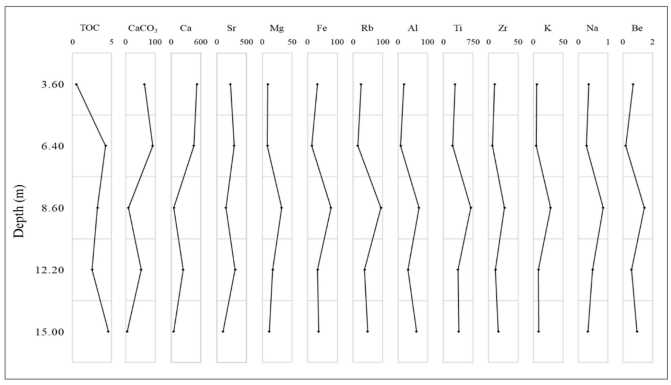
In the XRD analysis of sediments taken from 3.60 m and 12.20 m depth, calcite ($CaCO_3$), which is a drought proxy, shows dominant values.



Following the TOC (%) and $CaCO_3$ (%) analyses on the sediment samples collected from the paleo lake with proxy trap, a multi-element analysis was performed using ICP-MS on five reference levels representing humid and arid climatic periods. These five levels correspond to depths of 3.60, 6.40, 8.60, 12.20 and 15.00 metres. The analysis examined the vertical distributions of Ca, Sr, Na, Mg, Fe, Rb, K, Al, Ti, Zr, and Be, as well as their ratios to each other (Figure 10).

Figure 10

Distribution graphs of TOC, $CaCO_3$ and Ca, Sr, Na, Mg, Fe, Rb, K, Al, Ti, Zr, Be elements depending on depth.



The retention mechanism of elements is influenced by the fact that atoms with similar properties, such as ionic radii and electrical charges, tend to integrate into the same lattice structure, forming element associations. Ca and Sr, Rb and K, and Al and Ti cluster together (Zeng et al., 2013). High concentrations of Ca and Sr, along with elevated carbonate levels, are the most evident indicators of arid periods. In contrast, sediments formed under humid climatic conditions typically contain high amounts of Fe, Mg, and Rb (Fu & Wang, 2011).

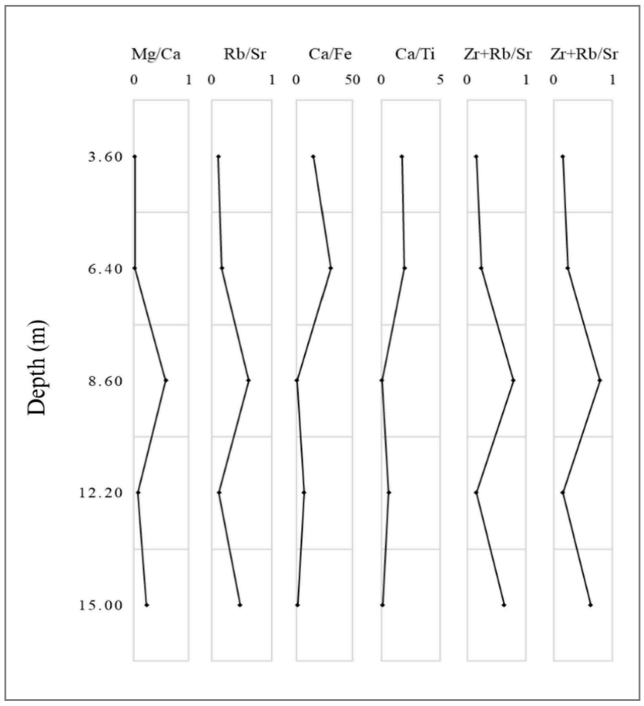
In this study, not only the percentage distribution of elements and the consistency of TOC (%) and $CaCO_3$ (%) data but also the ratios of Mg/Ca, Rb/Sr, Ca/Fe, Sr/Ca, Ti/Al, and Zr+Rb/Sr were considered (Figurer 11) as paleoclimate proxies (Yang et al., 2021; Ekoko et al., 2023). High Mg/Ca ratios, which are highly sensitive to climate fluctuations, often represent arid conditions, while low ratios represent humid conditions because Mg precipitates more easily in arid climates compared to Ca (Billups & Schrag, 2003). However, this pattern becomes invalid if K and Na are introduced into the precipitation process. When Na begins to precipitate in the environment, the Mg2+ and Ca2+ concentrations decrease, leading to a lower presence of Mg in the precipitation environment, as Mg is less reactive than Ca. Therefore, as long as Ca continues to precipitate, the Mg/Ca ratio decreases. In other words, high values of K and Na mixed with precipitation and a low ratio of Mg/Ca indicate arid conditions, while low values of K and Na and a high value of Mg/Ca reflect a humid climate (Ekoko et al., 2023).

Similarly, the concentration of Sr, which is known to cluster with Ca and increase due to evaporation-driven precipitation in arid conditions, remains low compared to Rb, a key detrital precursor element. The same trend applies to the Ca/Fe and Ca/Ti ratios (Ekoko Eric et al., 2023). If the Mg/Ca ratio is high, aragonite-dominated carbonate sedimentation occurs (Ries 2005; Balthasar & Cusack 2015). At a depth of 8.60 m, the increase in the Mg/Ca ratio indicates a hot and humid climate (Figurer 11). Likewise, major elements such as Si, Al, and Ti, along with the trace element Zr, which are reported to cluster together, have a detrital origin. Therefore, low Ti/Al ratios indicate humid conditions where chemical weathering is more intense, while high values indicate arid conditions (Figurer 11). Lower temperatures and a low Mg/Ca ratio result in $CaCO_3$ saturation and calcite-dominated sedimentation (Morse & Wang, 1997; Ries 2010). The low Mg/Ca ratio in the 3.60m, 6.40m, and 12.20m sediments indicates cool and arid climate conditions in the research region (Figurer 11).

The (Zr+Rb)/Sr ratio (Figurer 11) reflects the balance between the clastic (detrital) and carbonate components, serving as an indicator of the biogenic content of the sediment. Higher values are typically observed in the low-carbonated samples. The abundance of Zr signifies the presence of a relatively coarse, sandy siliciclastic material composed of quartz-rich grains, feldspars, and mafic minerals. Rb represents the density of the fine-grained and siliciclastic material. Sr is normally associated with carbonate minerals, particularly calcite and aragonite (Ekoko et al., 2023). Consequently, humid climates are characterised by a high Zr+Rb/Sr ratio, while arid climates are indicated by a low ratio, especially in environments with elevated Sr concentrations (Yang et al., 2021). At a depth of 8.60 m, the increase in the Zr+Rb/Sr ratio indicates a humid climate (Figurer 11).

Figurer 11

Binary element percentage distribution graph depending on the depth.

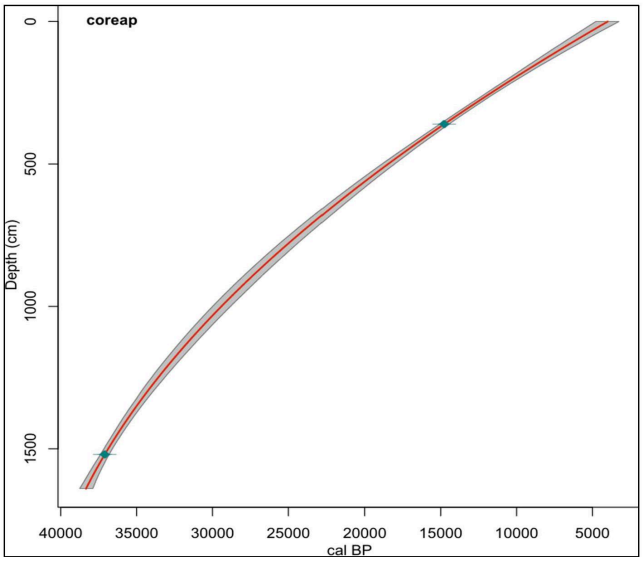


Accelerator mass spectrometry (AMS) radiocarbon dating was conducted on the samples taken from depths of 3.60 and 15.0 metres by the Marmara Research Centre of the Scientific and Technological Research Council of Turkey (TÜBİTAK). Based on the measured ^{14}C content in the samples, delta ^{13}C correction was conducted, and their ^{14}C ages were found to be 14.763 ±53 (BP) and 36.854 ±233 (BP), respectively (Stuiver & Reimer, 1993; Reimer et al., 2003).

Calibrated ages were determined with R Studio 4.4.2 with the "Clam.r" function (Blaauw, 2010; Blaauw, 2022), which is a non-Bayesian method, to produce the age-depth model (Figure 12). The red line represents the mean age, whereas the blue dots represent the AMS ^{14}C ages. The greyscale background shows the confidence interval. The depths of 6.40m, 8.60m, and 12.20m, where significant variations in proxy data were observed, correspond to approximately 23.707 ±548 years BP, 29.147 ±660 years BP, and 35.040 ±503 years BP, respectively. Each level discussed here reveals different depositional conditions subject to unique hydrological and sedimentological processes. The age-depth curve indicates higher sedimentation rates before 20–25 ka BP and lower rates in the recent past.

Figure 12

Age-depth model graph based on AMS ^{14}C data.



RESULTS AND DISCUSSION

The depth of 3.60 m had low TOC values but high $CaCO_3$ and correspondingly high Ca values. Although the similar oscillation of $CaCO_3$ and Ca implies that the carbonate was deposited via terrestrial transport (in feldspar), the Na and K values were not as high as expected (Figs. 5 and 6). Moreover, the presence of detrital precursor materials such as Mg, Fe, Rb, K, Al, Ti, and Zr with low representation indicates arid conditions characterised by slow chemical weathering (Jones et al., 2006; Kuzucuoğlu et al., 2011). Despite the increasing trend observed in Ca/Fe, Ca/Ti, Ti/Al, low Rb/Sr, Sr/Ca, and Zr+Rb/Sr ratios also align with the dry period data (Fig. 8). This inverse relationship between these element groups suggests that they were not transported together during a dry period, and the results can thus be attributed to evaporation rather than terrestrial flow. Considering the predominance of calcite, considered as a drought proxy in the previous section, the results confirm that hot-arid climatic conditions dominate the depth of 3.6 m.

Similar to 3.60 m, the depth of 6.40 m is characterised by high TOC and $CaCO_3$ and minimum values of Mg, Fe, Rb, K, Al, Ti, Zr, Na and Be. In dry conditions, higher calcium carbonate precipitation resulting from evaporation is observed, but there is a dramatic increase in the Ca/Fe and Ca/Ti ratios due to the low transport of Ti and Fe, indicating the most severe drought period within this phase. However, TOC, associated with high biological production as an indicator of paleo-productivity (Schoepfer et al., 2015), was higher than expected during this phase. This TOC enrichment, despite nutrient limitations in arid conditions, may be explained by the anoxic (oxygen-free)

and suboxic conditions at the sediment interface due to the cold and arid conditions (Tribovillard et al., 2006).

At the depth of 8.60m, the Ca was minimum despite the low $CaCO_3$ and high TOC. This excessive detrital material input indicates that the period was characterised by humid conditions. While Ca, which moves in the opposite direction from other proxies, shows that precipitation occurred through evaporation, other proxies, including the high levels of elements such as Fe, Mg, Rb, Al, Ti, and Zr by terrestrial transport, the high Mg/Ca ratio due to the effect of Na and K mixed into precipitation, and the high Zr+Rb/Sr ratio controlling the transport, confirm the presence of a rainy climate.

Low TOC and high $CaCO_3$ were observed at a depth of 12.20 m, and the inconsistency of $CaCO_3$ and Ca as well as the predominance of calcite reveal that the lime was not deposited by terrestrial transport. Furthermore, the amounts of elements known to be transported by precipitation, such as Fe, Mg, Rb, Al, Ti, and Zr, were low (compared to 8.60 and 15.00). Similarly, the Zr+Rb/Sr ratio, which controls the detrital material input, was also relatively low. This pattern, which is commonly observed in environments with slow chemical weathering (Oliva et al., 2003), provides evidence of arid conditions with relatively low precipitation at a depth of 12.20.

Similar to the depth of 8.60m, at the depth of 15.0m, high TOC, low $CaCO_3$, and correspondingly low levels of Ca and Sr were observed. These observations that cold conditions with very low evaporation prevailed. The values of Fe, Mg, Rb, Al, Ti, Zr were relatively low compared to the extremely humid level of 8.60, but higher than the depths of 3.60, 6.40, and 12.20, which are known to be arid. Several geochemical index ratios further support the interpretation of cold and rainy conditions based on high Rb/Sr, Sr/Ca, Mg/Ca, Zr+Rb/Sr and low Ca/Fe, Ca/Ti, Ti/Al (Gürbüz et al., 2024), albeit less humid than at 8.60.

Sampling at 10-cm intervals may be considered as low-resolution; also, the number of radiometric dating analyses was limited to only 2, and the chronology is built on the age-time graph, which constitutes the potential weaknesses of this study. Analysis of fossil pollen or other biotic proxies that would significantly contribute to this research was excluded in the evaluation because they are still ongoing. Once the analyses of fossil pollen and other biotic proxies are completed, their results will be evaluated for publication. The strength of this study is that it is the first study that identifies paleoclimatic changes and the timing of these changes in the region through the proxy elements selected for analysis (Ca, Sr, Na, Mg, Fe, Rb, K, Al, Ti, Zr, Be), autigenically-deposited calcium carbonate ($CaCO_3$), total organic carbon (TOC), and mineral crystal structure.

CONCLUSION

This study analysed 147 samples taken at 10-cm intervals from the 17-m drilling core and identified five reference levels characterised by different temperature and precipitation conditions. The depths of 3.60 m and 12.20m are marked by high $CaCO_3$ and decreased total organic carbon, explaining the low decomposition rate and arid conditions. High concentrations of Fe, Ti, K, Rb, Be, and Zr, as well as high levels of total organic carbon at 8.60 m and 15.00m, indicate humid conditions. On the other hand, the low ratios of Al and Ti with an elevated Ca at a depth of 6.40 m are associated with a cold-dry period. This study identifies two periods of relatively hot-arid conditions with low detrital input, two periods of cold-humid conditions, and one period of cold-dry conditions based on geochemical data. It is remarkable that although the depth levels of 15.00m, 12.20m, and 8.60m are located within MIS-3, they are characterised by relatively different temperature and precipitation indicators compared to each other. The depth of 6.40 m in MIS-2 supports the effect of low temperature and precipitation conditions and the Glacial Maximum in Eastern Thrace. The depth of 3.60m, dated to the interglacial period transition following MIS-2, marks a phase of increasing ambient temperatures.

Acknowledgments

This study was funded by the Scientific Research Coordination Unit (BAP) of Istanbul University (Project number: SDK-2023-38990). The researchers would like to express their gratitude to BAP for their support.

Peer Review Externally peer-reviewed.
Conflict of Interest The author have no conflict of interest to declare.
Grant Support The author declared that this study has received no financial support.

Author Details

Özlem Yurtseven Uyar
[1] Istanbul University, Institute of Social Sciences, Department of Geography, Istanbul, Türkiye.
0000-0002-9097-2449 ozlemyurtsevenuyar@ogr.iu.edu.tr

Hüseyin Turoğlu
[2] Istanbul University, Department of Geography, İstanbul, Türkiye.
0000-0003-0173-6995

AhmetEvren Erginal
[3] Çanakkale Onsekiz Mart University, Department of Geography Education, Çanakkale, Türkiye.
0000-0002-3112-5258

Nurettin Yakupoğlu
[4] Istanbul Technical University, Faculty of Mines, Geological Engineering, İstanbul, Türkiye.
0000-0003-2837-5771

REFERENCES

Balthasar, U., & Cusack, M. (2015). Aragonite–calcite seas—Quantifying the grey area. *Geology*, 43(2): 99–102. doi: 10.1130/G36293.1

Billups K., Schrag, D.P. (2003). Application of benthic foraminiferal Mg/Ca ratios to questions of Caenozoic climate change. *Earth and Planetary Science Letters*, 209(1-2): 181-195. doi:10.1016/S0012-821X(03)00067-0

Birks, H. H. & Birks, H. J. B. (2006). Multi-proxy studies in palaeolimnology. Vegetation History and Archaeobotany, 15: 235-251. https://doi.org/10.1007/s00334-006-0066-6

Blaauw M. (2010). Methods and code for 'classical'age-modelling of radiocarbon sequences. *Quaternary Geochronology*, 5 (5): 512-518. https://doi.org/10.1016/j.quageo.2010.01.002

Blaauw M. (2022). *CLAM: classical age-depth modelling of cores from deposits.*

Çağatay M., Ögretmen N., Damcı E., Stockhecke M, Sancar Ü, Eriş K., Özeren S. (2014). Lake level and climate records of the last 90 ka from the Northern Basin of Lake Van, eastern Turkey. *Quaternary Science Reviews*, 104: 97-116. doi:10.1016/j.quascirev.2014.09.027

Danladi, I. B. Akçer-Ön, S., Litt, T., Ön, Z.B. & Wacker, L. (2023). A Late Holocene climate reconstruction from the high-altitude Lake Gölcük sedimentary records, Isparta (SW Anatolia). *Quaternary Research. 115*: 120-133. https://doi.org/10.1017/qua.2023.26

Dean W. (1999) - The carbon cycle and biogeochemical dynamics in lake sediments. *Journal of Paleolimnology,* (21): 375-393. https://doi.org/10.1023/A:1008066118210

Dökmeci, A. H. (2017). Ergene Nehri Havzasında ağır metal kirliliğinin halk sağlığı açısından değerlendirilmesi [Evaluation of heavy metal pollution in the Ergene River Basin from a public health perspective]. *Turkish Journal of Public Health*, 15(3): 212–221. https://dergipark.org.tr/en/download/article-file/399633

Eastwood W., Leng M., Roberts N., Davis B. (2007). Holocene climate change in the eastern Mediterranean region: a comparison of stable isotope and pollen data from Lake Gölhisar, southwest Turkey. *Journal of Quaternary Science*, 22 (4): 327-341. https://doi.org/10.1002/jqs.1062

England A., Eastwood W., Roberts C., Turner R., Haldon J. (2008). Historical landscape change in Cappadocia (central Turkey): A palaeoecological investigation of annually laminated sediments from Nar lake. *The Holocene*, 18 (8): 1229-1245. https://doi.org/10.1177/095968360809

Ekoko Eric B., Adama A., Etutu M., Njinto Kwankam F., Salomon B., Esue M. (2023) Paleoclimate characteristics of source area weathering and metallogenic implication of cretaceous black shales in the Mamfe basin, (SW Cameroon): Evidence from lithogeochemistry. *Heliyon*. 9(6):e17142. doi:10.1016/j.heliyon.2023.e17142

Erginal A.E., Akbaş A., Kaya H., Çakır Ç., Karabıyıkoğlu, M. (2017). Belirteç element dağılımlarına göre Küçükçekmece Gölü'nde son 700 yıllık iklimsel salınımların izleri. *Uluslararası Jeomorfoloji Sempozyumu (12-14 Ekim 2017) Bildiriler Kitabı*: 649-650. Elazığ.

Febrida R., Setianto S., Herda E., Cahyanto A., Joni I.M. (2021). Structure and phase analysis of calcium carbonate powder prepared by a simple solution method. *Heliyon*, 7(11): e08344. doi:10.1016/j.heliyon.2021.e08344

Fu F., Wang Q. (2011). Removal of heavy metal ions from wastewaters: a review. *Journal of Environmental Management*, 92(3): 407-418. https://doi.org/10.1016/j.jenvman.2010.11.011

Gayantha, K., Routh, J., & Chandrajith, R. (2017). A multi-proxy reconstruction of the late Holocene climate evolution in Lake Bolgoda, Sri Lanka. *Palaeogeography, Palaeoclimatology, Palaeoecology*, 473: 16-25. https://doi.org/10.1016/j.palaeo.2017.01.049

Gürbüz, K., Mutlu, H., Ünal, İ. E., Uysal İ.T., Zhao J.X. (2024). New paleohydroclimate record of the MIS 5e/5d transition from Yelini Cave, central Anatolian region of Türkiye. *Quaternary Research*, 118, 162-179. https://doi.org/10.1017/qua.2023.56

Gürgey, K. (2009). Geochemical overview and undiscovered gas resources generated from Hamitabat petroleum system in the Thrace Basin, Turkey. *Marine and Petroleum Geology*, 26(7): 1240–1254. doi:10.1016/j.marpetgeo.2008.08.007

Hedges, J. I., & Keil, R. G. (1995). Sedimentary organic matter preservation: an assessment and speculative synthesis. *Marine Chemistry*, (49/2-3), s. 81-115.

Hu X., Wei J., Du Y., Xu L., Wang H., Zhang G., Ye W., Zhu L. (2010). Regional distribution of the Quaternary Red Clay with aeolian dust characteristics in subtropical China and its paleoclimatic implications. *Geoderma*, 159(3-4):317-334. https://doi.org/10.1016/j.geoderma.2010.08.008

Inkaya, S., Caner, H., Woodbridge, J., Turoglu, H., Makineci, E., Ozturna, A. G., Avci, M. (2025). How have Mediterranean peatlands changed in response to human influence during the Late Holocene? A case study from the Gölbaşı peatlands, Türkiye. *Quaternary International*, 732: 109806.

Jin Z., Cao J., Wu J., Wang S. (2006). A Rb/Sr record of catchment weathering response to Holocene climate change in Inner Mongolia. *Earth Surface Processes and Landforms*, 3 (3): 285-291. https://doi.org/10.1002/esp.1243

Jin Z., Wang S., Shen J., Zhang E., Li F., Ji J., Lu X. (2001). Chemical weathering since the little ice age recorded. In: Lake sediments: a high-resolution proxy of past climate. *Earth Surface Processes and Landforms*, 26(7): 775-782. doi:10.1002/esp.224

Jones M., Roberts C. (2008). Interpreting lake isotope records of Holocene environmental change in the Eastern Mediterranean. *Quaternary International*, 181: 32-38. https://doi.org/10.1016/j.quaint.2007.01.012

Jones M., Roberts C., Leng M., Türkes M. (2006). A high-resolution late Holocene lake isotope record from Turkey and links to North Atlantic and monsoon climate. *Geology*, 34(5): 361-364. https://doi.org/10.1130/G22407.1

Kılıç N.K., Caner H., Erginal A.E., Ersin S., Selim H., Kaya H. (2018). Environmental changes based on multi-proxy analysis of core sediments in Lake Aktaş, Turkey: preliminary results *Quaternary International*, 486: 89-97. https://doi.org/10.1016/j.quaint.2018.02.004

Kıyak N., Erginal A.E. (2010). Optical Stimulated Luminescence Dating Study of Eolianite on the Island of Bozcaada, Turkey: Preliminary Results *Journal of Coastal Research*, 26(4): 673-680. https://doi.org/10.2112/08-1169.1

Kuzucuoğlu C., Dörfler W., Kunesch S., Goupille F. (2011). Mid- to late-Holocene climate change in central Turkey: The Tecer Lake record. *The Holocene*, 21(1): 173-188. https://doi.org/10.1177/0959683610384

Łachacz, A., Kalisz, B., Mendyk, Ł., Gawlik, J. (2024). Holocene lake sediments as the parent material of soil. *Soil Science Annual*, 75(1): 1–14

Leroy S., Schwab M.J., Costa P. (2010). Seismic influence on the last 1500-year infill history of Lake Sapanca (North Anatolian Fault, NW Turkey). *Tectonophysics*, 486: 15-27. https://doi.org/10.1016/j.tecto.2010.02.005

Liu J., Clift P., Yan W., Chen Z., Chen H., Xiang R., Wang D. (2014). Modern transport and deposition of settling particles in the northern South China Sea: sediment trap evidence adjacent to Xisha trough, deep Sea Research Part I. *Oceanographic Research Papers*, 93:145-155. https://doi.org/10.1016/j.dsr.2014.08.005

Meyers, P. A. (2003). Applications of organic geochemistry to paleolimnological reconstructions: a review. *Organic Geochemistry*, 34(7): 889-913.

Minyuk P., Borkhodoev V., Wennrich V. (2014). Inorganic geochemistry data from Lake El'gygytgyn sediments: marine isotope stages 6-11. *Climate of the Past*, 10: 467-485. https://doi.org/10.5194/cp-10-467-2014

Ocakoglu F.K. (2013) - Early to Mid-Holocene Lake level and temperature records from the terraces of Lake Sünnet in NW Turkey. *Palaeogeography, Palaeoclimatology, Palaeoecology*, 369: 175-184. doi:10.1016/j.palaeo.2012.10.017

Özdoğan, E. (2011a). Settlement Organization and Architecture in Aşağı Pınar. Early Neolithic Layer 6. Beginnings – New Research in the Appearance of the Neolithic between Northwest Anatolia and the Carpathian Basin içinde, (Ed: Krauss R.), pp. 213-223, Verlag Marie Leidorf.

Özdoğan, E. (2011b). Settlement Organization and Architecture in Aşağı Pınar / 2011 Beginnings - New Research in the Appearance of the Neolithic between Northwest Anatolia and the Carpathian Basin, Papers of the International Workshop 8th, 214-223, Istanbul: Verlag Marie Leidorf GmbH.

Özdoğan, E. (2015). Current Research and New Evidence for the Neolithization Process in Western Turkey. *European Journal of Archaeology*, 18(1): 33-59

Oliva P., Viers J., Dupré b. (2003). Chemical weathering in granitic environments. *Chemical Geology*, 202 (3-4): 225-256. doi:10.1016/j.chemgeo.2002.08.001

Ries, J. B. (2005). Aragonite production in calcite seas: effect of seawater Mg/Ca ratio on the calcification and growth of the calcareous alga Penicillus capitatus. *Paleobiology*, 31(3): 445–458. https://doi.org/10.1666/0094-8373(2005)031[0445:APICSE]2.0.CO;2

Ries, J. B. (2010). Geological and experimental evidence for secular variation in seawater Mg/Ca and implications for carbonate sedimentation. *Biogeosciences*, 7: 2795–2849. doi:10.5194/bg-7-2795-2010

Roberts N., Reed J., Leng M., Kuzucuoğlu C., Fontugne M., Bertaux J., Hunt E. (2001). The tempo of Holocene climatic change in the eastern Mediterranean region: New high-resolution crater- lake sediment data from central Turkey. *The Holocene*, 11(6): 721-736. https://doi.org/10.1191/09596830195744

Roeser P., Franz S., Litt T. (2016). Aragonite and calcite preservation in sediments from Lake Iznik related to bottom lake oxygenation and water column depth. *Sedimentology*, 63 (7): 2253-2277. https://doi.org/10.1111/sed.12306

Roeser P., Franz S., Litt T., Ülgen U., Hilgers A., Wulf S., Wennrich V., Akçer Ön S., Viehberg F.A., Çağatay M.N., Melles M. (2012). Lithostratigraphic and geochronological framework for the paleoenvironmental reconstruction of the last ~36 ka cal BP from a sediment record from Lake Iznik (NW Turkey). *Quaternary International*, 274: 73-87. doi:10.1016/j.quaint.2012.06.006

Roper, D. C. (1979). *The Method and Theory of Site Catchment Analysis: A Review II*. New York: Academic Press.

Rossi C., Lozano R. (2016). Hydrochemical controls on aragonite versus calcite precipitation in cave dripwaters. *Geochimica et Cosmochimica Acta*, 192: 70-96. doi:10.1016/j.gca.2016.07.021

Rostási Á., Rácz K., Fodor M., Topa B., Molnár Z., Weiszburg T.G.; Pósfai M. (2022). Pathways ofcarbonatesediment accumulation in a large, shallow lake. *Frontiers in Science*, 10: 1067105. doi:10.3389/feart.2022.1067105

Reimer P.J., Bard E., Bayliss A., et al. (2013). Selection and Treatment of Data for Radiocarbon Calibration: An Update to the International Calibration (IntCal) Criteria. *Radiocarbon*, 55(4):1923-1945. doi:10.2458/azu_js_rc.55.16955

Sebag, D., Debret, M., M'voubou, M., Obame, R.M., Ngomanda, A., Aslisly, R., Bentaleb, I., Disnar, J-R., Giresse, P. (2013). Coupled Rock-Eval pyrolysis and spectrophotometry for lacustrine sedimentary dynamics: Application for West Central African rainforests (Kamalété and Nguène lakes, Gabon). *The Holocene*, 23(8): 1173–1183.

Schlichting, E. & Blume, H. (1966) *Bodenkundliches Praktikum*. Hamburg: Parey-Verlag

Schoepfer S.D., Shen J., Wei H., Tyson R.V., Ingall E., Algeo T.J. (2015) - Total organic carbon, organic phosphorus, and biogenic barium fluxes as proxies for paleomarine productivity. *Earth-Science Reviews*, 149: 23-52. https://doi.org/10.1016/j.earscirev.2014.08.017

Schroeter, N., Toney, J., Lauterbach, S., Kalanke, J., Schwarz, A., Schouten, S. &Gleixner, G. (2020). How to Deal With Multi-Proxy Data for Paleoenvironmental Reconstructions: Applications to a Holocene Lake Sediment Record from the Tian Shan, Central Asia. *Frontiers in Earth Science*. 8: 353, https://doi.org/10.3389/feart.2020.00353

Sezen E., & Karakaş Z.S. (2025). Newly identified uranyl vanadate mineral formation in the Thrace Basin, NW Türkiye: Insights into identification and origin of carnotite and tyuyamunite minerals. *Bulletin of the Mineral Research and Exploration* 177: 11-22. https://doi.org/10.19111/bulletinofmre.1554734

Strakhovenko, V., Subetto, D., Ovdina, E., Belkina, N. & Efremenko, N. (2020). Distribution of Elements in Iron-Manganese Formations in Bottom Sediments of Lake Onego (NW Russia) and Small Lakes (Shotozero and Surgubskoe) of Adjacent Territories. *Minerals*, (10/5), 440

Stuiver, M. & Reimer, P.J. (1993). Extended 14C database and revised CALIB 3.0 14C age calibration program. *Radiocarbon*, 35(1): 215-230.

Smith, H. & Weldon, M. (1941). A comparison of some methods for the determination of soil organic matter. *Soil Science Society of America*, 5:177-182.

Turoğlu H. (2007). Yoncatepe (Van) Arkeolojik Sahası Paleo-Landuse Çalışmalarında Fiziki Coğrafya Verileri. *Türkiye Kuvaterner Sempozyumu TURQUA (VI)*: 76-87. İstanbul.

Turoğlu H. (2011). *Reconstructing the paleolanduse of Urartian period for Yoncatepe Archaeologic Site (Van, Turkey)*. Çantay Kitabevi, İstanbul

Turoğlu H., Caner H., Yüksel F.A., Sarı E. (2008). Erek Dağı Çevresi (Van) Paleocoğrafya Özelliklerine Ait Durgun Su Çökellerinden Üretilen Veriler. *Ulusal Jeomorfoloji Sempozyumu*, (p. 430- 434). Çanakkale.

Tribovillard N., Algeo T.J., Lyons T., Riboulleau A. (2006). Trace metals as paleoredox and paleoproductivity proxies: an update. *Chemical Geology*, 232(1-2): 12-32. https://doi.org/10.1016/j.chemgeo.2006.02.012

Vita-Finzi, C. (1978). *Archaeological Sites in Their Setting*. London: Thames and Hudson.

Vita-Finzi, C., Higgs, E., Sturdy, D.J., Tippett, H. (1970). Prehistoric Economy in the Mount Carmel Area of Palestine: Site Catchment Analysis. *Proceedings of the Prehistoric Society*, 36: 1-37.

Von Gunten L., Grosjean M., Rein B., Urrutia R., Appleby P. (2009). A quantitative high-resolution summer temperature reconstruction based on sedimentary pigments from Laguna Aculeo, central Chile, back to AD 850. *The Holocene*, 19 (6): 873-881. https://doi.org/10.1177/0959683609336

Yang H., Zhao Y., Cui Q., Ren W., Li Q. (2021). Paleoclimatic indication of X-ray fluorescence core-scanned Rb/Sr ratios: A case study in the Zoige Basin in the eastern Tibetan Plateau. *Science China Earth Science*, 64: 80-95. doi:10.1007/s11430-020-9667-7

Zeng Y., Chen J., Xiao J., Qi L. (2013). Non-residual Sr of the sediments in Daihai Lake as a good indicator of chemical weathering. *Quaternary Research*, 79(2): 284-291. https://doi:10.1016/j.yqres.2012.11.010